



S. Suzuki



G.A. Dulk

CHAPTER 13. TYPE II BURSTS

G.J. Nelson and D.B. Melrose

13.1 INTRODUCTION

In this chapter we consider in detail the Type II burst, which has already been briefly discussed in Chapters 1 and 3. We first review the evidence for identifying these events as plasma emission associated in some way with magnetohydrodynamic (MHD) shock waves in the corona. We then present the evidence of associations between Type II bursts and other solar disturbances, followed by a detailed description of the observed features of the Type II radio emission itself. We go on to apply this observational data to the detailed interpretation of Type II bursts. In this context we discuss both the emission mechanism itself and the nature of the coronal disturbances which excite the bursts. Finally we outline possible acceleration processes which can produce the energetic particles which are clearly required to account for the observed radio emission.

Evidence for the plasma hypothesis

The most direct evidence for the plasma hypothesis for Type II bursts is provided by positional data on moving sources. The frequency drift rate for Type II bursts implies a radial speed between 200 and 2000 km s⁻¹, and one would therefore expect observations to show that a source at the limb moves outwards at a speed in this range. The first evidence that this is so came from swept-lobe, swept-frequency interferometry (Wild *et al.* 1959b; Smerd *et al.* 1962). Multi-frequency radio-heliograph observations have subsequently confirmed the outward motion of the sources. The early observations also showed that the motion of Type II sources is not always radial; Weiss (1963a) detected tangential motions at up to 2000 km s⁻¹.

Other evidence for the plasma hypothesis is indirect and is based on the fact that in several important respects Type II bursts have properties similar to those of Type III bursts; it is generally accepted that the latter are of plasma-wave origin (see Chapter 12). Thus Type II bursts, like Type III bursts, often show two harmonically related bands with an instantaneous frequency ratio slightly less than 2:1; this structure is a signature of plasma emission (see Chapter 1). Furthermore, Type III emission has characteristic polarization features, and these are also found to occur in herringbone Type II bursts (Section 13.3).

Nelson, G. S., & Melrose, D. 1985, in *Solar Radio Physics*, ed. D. J. McLean, & N. R. Labrum (Cambridge: Cambridge Univ. Press), 333

MHD shock as the exciting agency

The two earliest suggestions for the exciting agency for Type II bursts were (a) a stream of energetic ions (Wild 1950a), and (b) a gas-dynamic shock (Wild *et al.* 1954b). Both encountered difficulties. The major difficulty with suggestion (a) is the high ion velocity which is necessary for the generation of the Langmuir waves required for plasma emission. A stream of charged particles is unstable to Langmuir waves only if the streaming speed exceeds the thermal speed V_e of electrons by a factor greater than three. In the corona however $V_e \approx 4000 \text{ km s}^{-1}$, and so a stream at $\leq 2000 \text{ km s}^{-1}$ (the upper limit of observed Type II speeds) would not produce any plasma emission. The main difficulty with suggestion (b) is related to the very low collision frequency in the corona. For a particle at $\sim 1000 \text{ km s}^{-1}$ the collisional mean free path is $\sim 10^6 \text{ km}$. Under these conditions a gas-dynamic shock would have a thickness in excess of a solar radius and therefore would not be expected to produce radiation confined to a narrow frequency band. The low sound speed ($\sim 150 \text{ km s}^{-1}$) in the corona also requires unreasonably high Mach numbers (up to 10) for a gas-dynamic shock moving at the speed of the Type II exciters.

It was suggested by Uchida (1960) and Wild (1962) that the exciting agency is more likely to be an MHD shock. Such a shock has a velocity greater than that of a fast MHD wave, i.e.

$$V_{\text{shock}} > \left[V_A^2 + C_S^2 - \frac{V_A^2 C_S^2 \cos^2 \theta}{V_A^2 + C_S^2} \right]^{1/2}, \quad (1)$$

where V_A and C_S are the Alfvén and sound velocities respectively and θ is the angle between the wave normal and the magnetic field direction. In the corona $V_A \gg C_S$, so that eq. (1) reduces to $V_{\text{shock}} > V_A$. As argued below, an MHD-like disturbance is consistent with many observations. An MHD shock can propagate at any angle to the magnetic field, and the shock properties are only weakly dependent on this angle. Because of the low collision frequency, shocks in the corona must be collisionless, rather than collision-dominated. The theory of collisionless MHD-like shocks was developed through the 1960s and 1970s, and the progressive changes in ideas have had a dominant influence on the development of theories of Type II emission. This topic is discussed further in Section 13.6.

13.2 ASSOCIATION OF TYPE II BURSTS WITH OTHER SOLAR DISTURBANCES

H α flares

Type II bursts are closely associated with flares. For more than 90% of these bursts a corresponding flare is recorded; the remainder may all be due to flares which are not seen (usually because they are behind the solar limb). On the other hand, not all flares produce Type II bursts. Only 30% of importance 2 and 3 flares produce Type II bursts and the incidence is proportionately much less for smaller flares ($\sim 7\%$

for importance 1 and $< 0.3\%$ for sub-flares (C.S. Wright, personal communication)). However, small flares, because they are by far the most numerous, actually produce the majority of Type II bursts; 40% of the latter are associated with sub-flares, 40% with importance 1 and only 20% with flares of importance greater than 1 (Dodge 1975; Wright 1980). It has also been found that flares which produce energetic proton events in the interplanetary medium tend to produce Type II events. This at once suggests that Type II bursts are associated with an enhanced efficiency either of the acceleration of protons or of the escape of accelerated protons. The association of Type IV and flare continuum emission with many Type II bursts offers further support for the suggestion that acceleration of particles (in this case of electrons to mildly relativistic speeds) is associated with Type II events.

Moreton waves

Early evidence for the association of Type II bursts with MHD shock waves came from the interpretation of Moreton waves (Moreton 1960). Films of the Sun's disk photographed in the wings of the $H\alpha$ line sometimes show a curved disturbance spreading out across the chromosphere from the site of a flare at $\sim 1000 \text{ km s}^{-1}$. The accepted interpretation is in terms of Uchida's (1968) 'sweeping skirt' model. The idea is that an MHD disturbance in the corona is refracted towards the regions of low Alfvén speed V_A , where the disturbance is focused and strengthened. The upper layer of the chromosphere has a lower value of V_A than the overlying corona, and hence the disturbance should be strong near the top of the chromosphere. Because of the Doppler shift the moving material associated with this strong disturbance is visible in the wings of the $H\alpha$ line. There is a close correlation between flares which produce Moreton waves and flares which produce Type II bursts, suggesting that these are two manifestations of the same MHD disturbances (Wild 1969a; Uchida *et al.* 1973).

Coronal transients

It has long been known that mass is ejected from the Sun following sprays and eruptive prominences. The white light coronagraph on Skylab led to a clear identification of coronal transients associated with such ejections (Gosling *et al.* 1976; see Section 4.12). It also led to the identification of a second class of coronal transients associated directly with flares. These flare-related events are usually much faster (360 to 1200 km s^{-1}) than the eruptive prominence transients (100 to 600 km s^{-1}). Gosling *et al.* found that nearly all transients with speeds $> 400 \text{ km s}^{-1}$, whether they are related to flares or to eruptive prominences, are associated with metrewave Type II and Type IV emission. More recent studies of the relation between coronal transients, Type II bursts and other flare phenomena, using satellite-borne white light coronagraphs, suggest a more complex situation. Sheeley *et al.* (1984), using Solwind observations from 2.5 to $10 R_\odot$, found the following associations.

1. The 41% of coronal transients which were accompanied by Type II bursts had speeds $>400 \text{ km s}^{-1}$, and were associated with long-lived soft X-ray events (3 h on the average) and interplanetary shocks.
2. The remaining 59% of coronal transients which were not accompanied by Type II bursts were equally divided into groups with speeds faster and slower than 455 km s^{-1} . Some of the fast transients in this group originated behind the limb, in which case any associated Type II emission may have been occulted. On the other hand, some originated from flares on the visible disk, where Type II bursts should have been observed if they occurred. Whether or not they were accompanied by Type II bursts, the fast transients were generally associated with interplanetary shocks.
3. 30% of all Type II bursts were not accompanied by coronal transients. These events were associated with short-lived (0.5 h) soft X-ray events but not with interplanetary shocks.

The average speed of all coronal transients reported by Sheeley *et al.* (1983) is $\sim 840 \text{ km s}^{-1}$. For the 24 Type II bursts reported by Roberts (1959) the average speed, based on frequency drift rates, is $\sim 500 \text{ km s}^{-1}$ for the Saito *et al.* (1977) density model for the corona, or $\sim 1000 \text{ km s}^{-1}$ for a model with densities 10 times higher. The similarity of the average speeds of the Type II bursts and transients again suggests the possibility of a close relation between the two phenomena. The estimates of Type II speed are, of course, subject to considerable error because of the uncertainty about which density model is applicable. Velocities derived from heliograph observations of source positions are even more uncertain because of the imperfectly known effects of coronal scattering and refraction and of ionospheric refraction.

One interpretation of these statistical results is that long-duration flares produce coronal transients, which, if they have speeds greater than the Alfvén speed ($\sim 400 \text{ km s}^{-1}$), set up piston-driven shocks which in turn produce Type II emission and interplanetary shocks. On the other hand, the more impulsive flares do not give rise to coronal transients but to blast waves (see Section 13.5) which produce Type II emission but decay without producing interplanetary shocks. Fast coronal transients which do not produce Type II emission presumably propagate through the corona in regions of high v_A . This situation can occur for piston-driven shocks whereas, according to Uchida (1960), blast waves would rapidly be refracted out of such high- v_A regions.

This interpretation is not however entirely consistent with more detailed observations of individual events. Wagner (1983), MacQueen (1980) and Stewart (1980) reviewed the results of simultaneous radio and SMM coronagraph observations of coronal transient events. In each of three such events the Type II sources were observed to be well inside the transient and certainly not ahead of it, as would be expected in the case of a piston-driven shock. Particularly convincing is the transient of 1980 June 29, which exhibited both a faint arc moving outward at

$>900 \text{ km s}^{-1}$ and a bright loop transient moving at $\sim 600 \text{ km s}^{-1}$. Both seem to have originated either prior to the impulsive flare or at a considerable height above the flare (Gary *et al.* 1983). The Type II burst observed at Culgoora probably did not arise from the fast-moving arc (for which the Mach number was found to be ~ 1.3 to ~ 3) nor even from the leading edge of the loop transient. Instead the Type II emission either arose from the edges of the loop transient, which were expanding sideways at a lower speed of $<200 \text{ km s}^{-1}$, or, more probably, was due to a blast wave, initiated by the impulsive flare, which then travelled outwards through the already moving transient material. At present there is no convincing explanation for the lack of a Type II burst in association with the arc or with the leading edge of the loop transient.

The detailed relation between coronal transients and Type II bursts remains therefore somewhat confused. The possibility (suggested by the Gary *et al.* (1983) observations) that there is no causal relation is consistent with the observation by Sheeley *et al.* (1984) that transients exist without Type II emission and vice versa.

13.3 GROUND-BASED OBSERVATIONS OF TYPE II BURSTS

In reviewing ground-based radio data on Type II bursts we subdivide the observations into three parts: features which were clearly identified before the advent of radioheliography; the additional information provided by the radioheliograph; and finally some recent results of observations with the spectropolarimeter.

Basic properties

The basic spectral properties of metrewave Type II bursts were summarized by Roberts (1959) and have been reviewed by McLean (1974, 1980). They are as follows:

1. *Slow drift.* The emission drifts from high to low frequencies at less than 1 MHz s^{-1} .
2. *Narrow bandwidth.* Typical instantaneous bandwidths for the drifting bands vary from a few megahertz to $\sim 100 \text{ MHz}$.
3. *Harmonic structure.* Approximately 60% of the bursts appear in harmonic bands (Fig. 13.1a). In the remainder it appears likely that the fundamental is not observed because it cannot propagate in the direction of the observer. An example with very little harmonic structure is shown in Figure 13.1(b). This is the spectrum of a Type II burst originating from a flare behind the limb. The emission is predominantly harmonic, although in this particular case weak fundamental emission is occasionally visible.
4. *Band splitting.* Many of the bursts show a secondary doubling of the bands (Fig. 13.1c); the splitting $\Delta f/f$ is $\sim 10\%$ in each of the fundamental and harmonic bands.

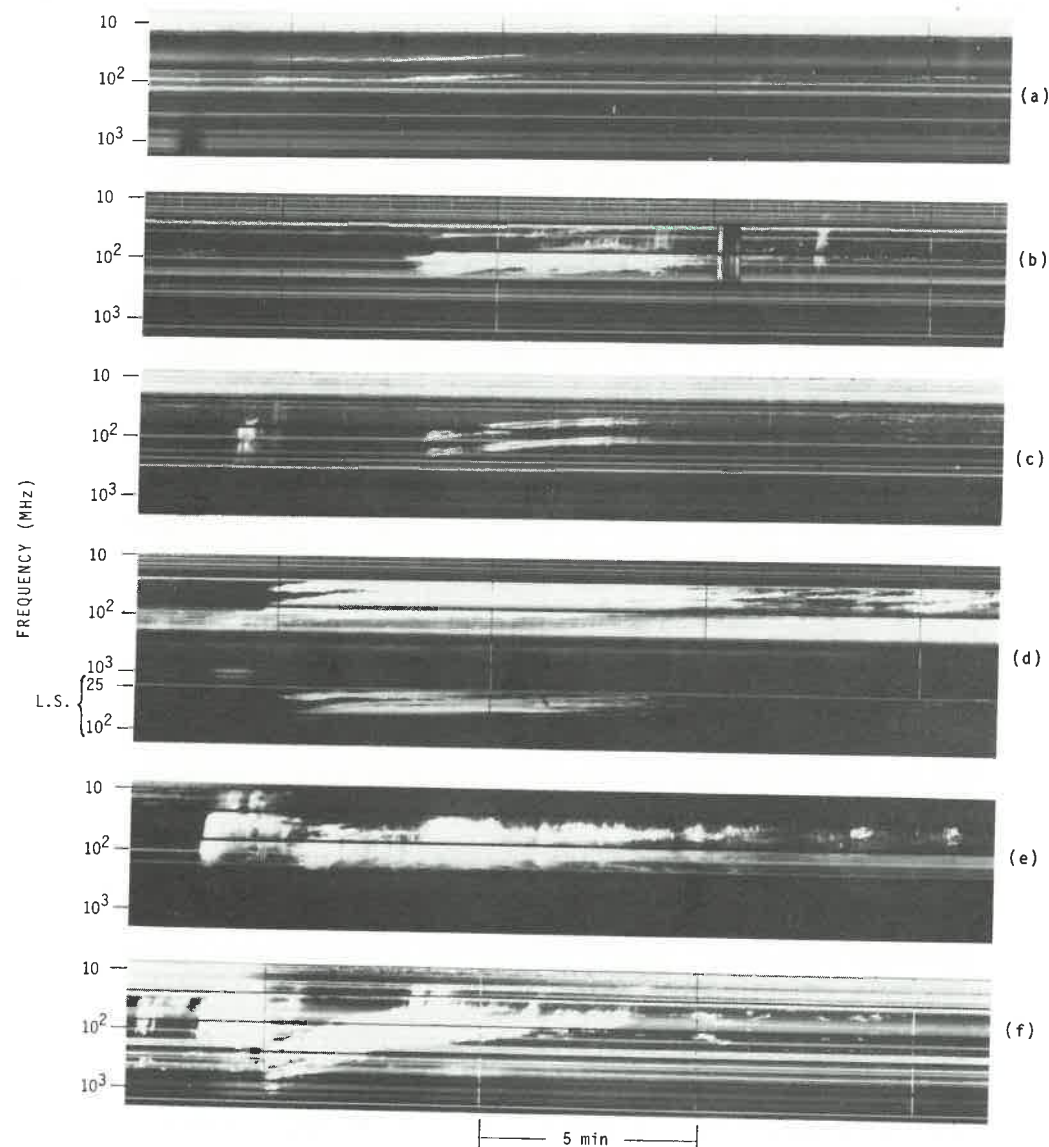


Fig. 13.1 - Examples of Type II bursts. (a) simple fundamental, harmonic event; (b) burst from behind the limb with almost no fundamental; (c) fundamental, harmonic and split-band structure; (d) multiple lanes (L.S. is a low-sensitivity recording); (e) herringbones; (f) Type II with very high starting frequency.

5. *Multiple lanes.* In some bursts there are several drifting bands or 'lanes' which are neither harmonically related nor consistent with simple band splitting. These are thought to be generated by separate disturbances propagating through the corona or by the interaction of a single extended disturbance with several different coronal structures. Some examples are shown in Figure 13.1(d).
6. *Herringbone structure.* In this variant of the Type II burst the characteristic slowly drifting band appears to be a source from which rapidly drifting, short-duration bursts emerge. Examples are shown in Figure 13.1(e). Sometimes rapidly drifting elements occur with both positive and negative slopes, so that the frequency-time structure has the appearance of a herringbone. At times the 'backbone' is entirely absent and only the rapidly drifting components are visible. A feature of herringbone bursts is that the drift rate is often very low. This may imply that the motion of the shock wave is nearly parallel to the solar surface and normal to magnetic field lines (Stewart & Magun 1980).
7. *Emission frequencies.* The starting frequency of the fundamental component is usually <150 MHz, although starting frequencies as high as 500 MHz have been observed (Fig. 13.1f). In most cases the Type II emission ends at a frequency above 20 MHz. However, in some cases, particularly in events with low starting frequencies (Robinson *et al.* 1984), the emission is observed down to frequencies at least as low as 100 kHz.
8. *Timing and duration.* With the exception of the very-long-lived interplanetary events the duration of a typical Type II burst is 5 to 15 min. These bursts always commence later than the associated flare; the lower the starting frequency, the longer the delay. Type II bursts with delays of only 2 min have been observed at very high frequencies, but more typical events start 5 to 20 min after the flare. This delay suggests that a disturbance initiated near the start of the flare produces radio emission in some distant region where conditions for shock formation exist.

Type II source sizes and locations

Early observations of Type II sources with the Culgoora radio-heliograph at 80 MHz (Kai & McLean 1968; Wild 1969a) showed that these sources are large ($\sim 0.5 R_{\odot}$). Observations at 43 MHz (Nelson & Robinson 1975) have subsequently revealed even larger sources ($\sim 1 R_{\odot}$). They are often circular or slightly elongated but are sometimes made of several different sub-sources around a wide arc centred on the site of the flare. An example is shown in Figure 13.2. For these multiple-source events the inferred angle of the emission cone of the shock wave is very large ($\sim 180^{\circ}$). The sub-sources vary rapidly on time scales as short as a second. It is thought that the different sub-sources correspond to different lanes of a multiple-lane spectrum.

As is the case with Type III bursts (see Section 12.2), observations of harmonic pairs at a single frequency do not show the expected

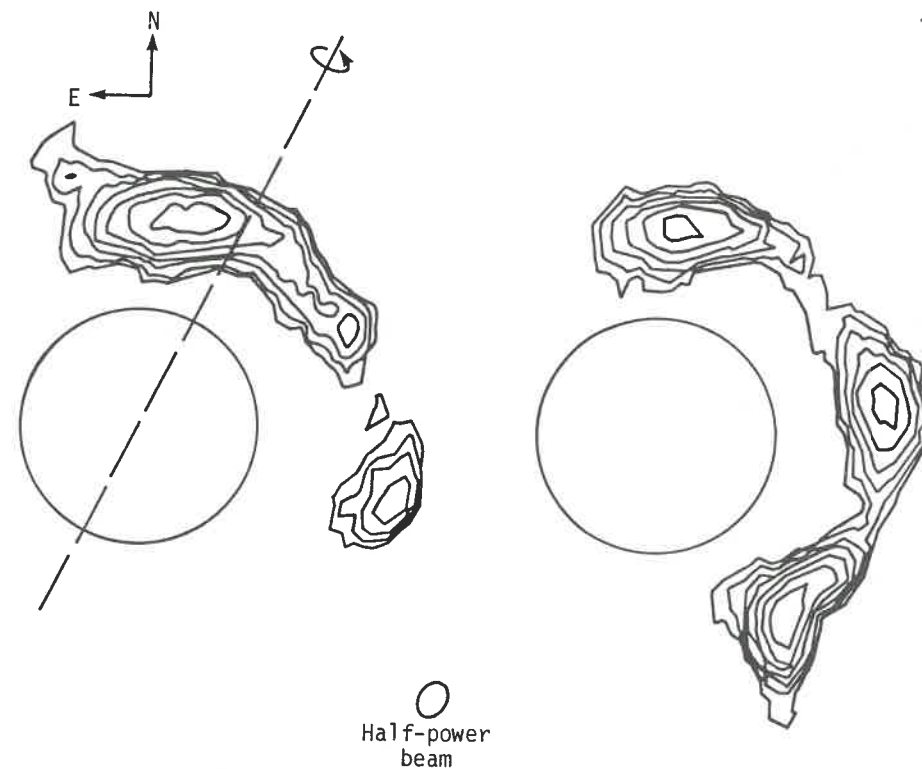


Fig. 13.2 - Culgoora radioheliograph observations of multiple elongated sub-sources of Type II emission. The two images are separated in time by 19 s. (After Smerd 1970.)

spatial separation between the sources. The fundamental emission at 80 MHz originates at the 80 MHz plasma level and the second harmonic emission at 80 MHz originates (at a later time) at the 40 MHz plasma level, i.e. at a much greater height. However, the observed separation is quite small; as a general rule, the apparent positions of the fundamental and second-harmonic sources at a given frequency are found to overlap. Early attempts were made to explain this discrepancy by refraction and by scattering off coronal irregularities (Steinberg *et al.* 1971; Riddle 1972b). A recent explanation in terms of ducting (Duncan 1979; see Section 10.4) seems more plausible.

Simultaneous observations of the fundamental emission $F(f)$ at a given frequency f and of the second harmonic $H(2f)$ at twice that frequency became possible with multi-frequency operation of the Culgoora radioheliograph. As might be expected from the near-coincidence of the $H(f)$ and $F(f)$ sources, the $H(2f)$ source is often much closer than the $F(f)$ source to the site of the flare (Nelson & Sheridan 1974).

The apparent size of Type II sources increases rapidly with decreasing frequency. Naively one might expect that the apparent sizes of $H(2f)$ and $F(f)$ sources would be similar and would correspond to the actual size of the source at the plasma level $f_p = f$. However, it is found that the two sources, $H(f)$ and $F(f)$, of emission at a given frequency f are of comparable size but that the $H(2f)$ source is much smaller than the $F(f)$ source. This also can be explained by the ducting model.

Brightness temperatures and flux densities

Although Type II bursts often exhibit large fluctuations in intensity with time and frequency, usually the maximum brightness temperature first increases with decreasing frequency and then decreases. Most Type II bursts decay completely before reaching 20 MHz; some however continue further, to become interplanetary Type II bursts with brightnesses considerably below that of their coronal counterparts. This behaviour contrasts with that of Type III bursts, which continue to increase in brightness with decreasing frequency until the source is far into the interplanetary medium.

The brightness temperature varies enormously from event to event. One of the brightest Type II bursts observed at Culgoora occurred on 1982 December 15. It had maximum brightness temperatures of 4×10^{10} , 1×10^{11} , 8×10^{12} and 5×10^{11} K at 327, 160, 80 and 43 MHz respectively. The corresponding fluxes were 2250, 11,500, 290,000 and 16,000 s.f.u. At the other extreme, a Type II burst recorded on the high-sensitivity acousto-optical spectrograph at Culgoora and observed by the heliograph at 80 MHz had a maximum brightness temperature of $\sim 10^7$ K and a flux of ~ 1 s.f.u. According to the wave-ducting model (which incorporates scattering at the top of the duct) these brightness temperatures are lower limits to the intrinsic brightness temperature at the source.

Not a great deal has been published about the relative brightness of the components of harmonically related Type II sources. For events near or behind the limb the fundamental emission is strongly attenuated by propagation effects (e.g. Fig. 13.1b) and in many cases is not observed at all. Near disk centre the fundamental usually exceeds the harmonic in brightness (Nelson & Robinson 1975).

Probably the brightest features in Type II bursts are herringbones. Stewart & Magun (1980) reported 43 MHz herringbone features with brightness temperatures in excess of 10^{13} K.

Split-band sources

Nelson & Robinson (1975) reported observations of five harmonic split-band Type II bursts at two different frequencies (either 160 and 80 MHz or 80 and 43 MHz). In all cases the four bands H_U , H_L , F_U and F_L were observed, where U and L refer, respectively, to the upper and lower frequency components of the split bands. They found the following properties.

1. At a given frequency the U and L sources were circular, essentially the same size, and in the same position. At the fixed observing frequency the L band is observed earlier in time than the U band and so it is inferred that at a given time the L source is further from the Sun than the U source.
2. The maximum brightness temperature T_B varied widely from one event to another in the ranges 4.5×10^6 to 1.7×10^{10} K at 160 MHz, 1.9×10^7 to 3.7×10^{10} K at 80 MHz, and 1.4×10^{10} to 5.9×10^{11} K at 43 MHz. T_B increased with decreasing frequency.
3. In seven out of 11 cases the L source was brighter than the U source. The ratio $T_B(L)/T_B(U)$ averaged over all cases was 2.3.

Polarization of Type II bursts

Early observations showed that ordinary Type II bursts are usually unpolarized or only weakly polarized (Komesaroff 1958; Roberts 1959). However, the herringbone structure in some bursts was found to be quite strongly polarized, e.g. up to 70% (Stewart 1966).

Observations using the Culgoora spectropolarimeter (see Section 6.5) were reported by Suzuki *et al.* (1980) for 16 Type II bursts with herringbone structure. They compared the polarization: (a) of the forward-drift and reverse-drift components of the herringbone structure at the fundamental; (b) of the fundamental and harmonic components in the herringbone structure; and (c) of the backbone and the herringbone structure. They found the following.

1. There is little systematic difference in polarization between the forward and reverse-drifting fundamental components, although the former is on average slightly more strongly polarized. In individual events however the difference may be marked. The mean degree of polarization (~50%) is similar to that for fundamental Type III bursts.
2. The polarization of the second-harmonic herringbones is similar to that of harmonic Type III bursts (~15%), as illustrated in Plate 2.
3. The backbone component has weak polarization (similar to that of Type II bursts without herringbone structure) and the sense of polarization of the backbone is always the same as that of the herringbone.

These results are all consistent with the hypothesis that the herringbone structure is due to Type-III-like emission from electron streams escaping from the shock front.

13.4 OBSERVATIONS OF TYPE II EVENTS IN THE INTERPLANETARY MEDIUM

Detailed observations of Type II bursts in the interplanetary medium have been made fairly recently with instruments on the Voyager spacecraft (Boischot *et al.* 1980) and on ISEE-3 (Cane *et al.* 1982).

A related type of event, called an SA (shock-accelerated) event was also observed; this is thought to correspond to the herringbone structure observed at metre wavelengths (Cane *et al.* 1981). The difficulty of identifying Type II bursts unambiguously is apparent from the fact that Cane *et al.* (1982) found about one per month while Boischot *et al.* (1980) found eight in one particular month. The most detailed study is that by Cane *et al.* (1982) with ISEE-3, and we concentrate here on their results. We also summarize some ISEE-3 data on the properties of wave turbulence observed in association with interplanetary shocks.

ISEE-3 observations

ISEE-3 was located approximately at the libration point, 240 Earth radii from the Earth along the Earth-Sun line. The Sun was continuously observable and radio interference from terrestrial sources was low. The radio receivers provided data at 24 frequencies between 2 MHz and 30 kHz, which correspond to plasma levels between $\sim 10 R_\odot$ and ~ 1 AU from the centre of the Sun respectively.

As well as providing the radio spectrum of the Type II event itself, the data from the satellite include a record of the low-frequency continuum at frequencies below the local plasma frequency. The passage of the shock at the satellite can be detected by a sharp increase in the upper-frequency limit of this continuum (Hoang *et al.* 1980). The time of arrival of the shock at the Earth can be estimated from the onset time of the accompanying sudden commencement (SC) in geomagnetic activity. The time interval between the passage of the shock at the spacecraft and the SC provides an estimate of the component of shock velocity along the Sun-Earth line. If an independent value of the shock speed is available it is possible to estimate the inclination of the shock velocity vector to the Sun-Earth line and hence to the interplanetary magnetic field.

An example of an interplanetary Type II burst is illustrated in Figure 13.3.

Summary of results for interplanetary Type II bursts

1. The bursts are difficult to observe because often they are little brighter than the galactic background.
2. The intensity fluctuates, with brightenings lasting an hour or so.
3. The drift rate towards lower frequencies is several kilohertz per minute at 1 MHz and ~ 1 kHz min^{-1} at 300 kHz.
4. Type II events in the interplanetary medium correlate with Type II and/or Type IV events in the corona.
5. Relatively few interplanetary shocks are accompanied by Type II bursts; when the latter are present they occur ahead of the shock and cut off as the shock passes the spacecraft.

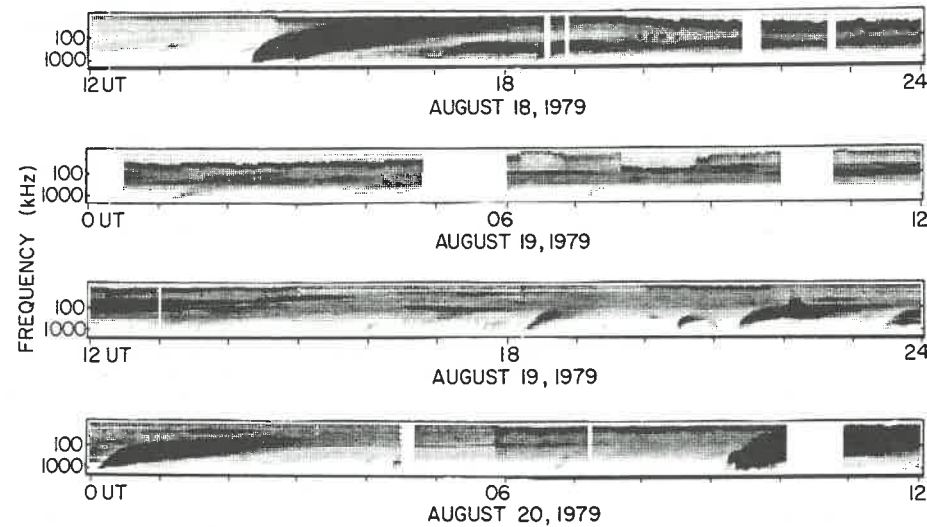


Fig. 13.3 - ISEE-3 dynamic spectra illustrating a kilometre Type II burst. The initiating flare occurred at ~ 1412 UT on 1979 August 18 and also produced a group of intense Type III bursts. The shock passed the spacecraft at ~ 0500 on August 20. The Type II radio emission is clearly visible at 1700 on August 18, through to 1400 on August 19. (From Cane *et al.* 1982.)

The observations of Cane *et al.* (1982) also give some indication of band splitting and of harmonic structure. They suggest that on some occasions a change from F to H takes place as the frequency decreases.

Shock-accelerated (SA) events

An example of the class of interplanetary radio event called SA (Cane *et al.* 1981) is shown in Figure 13.3. These bursts bear some resemblance to interplanetary Type III bursts. However, SA events are more intense and of longer duration than Type III bursts and, more important, the metrewave events with which they are associated are of Type II and not Type III. More specifically, SA events are correlated with herringbone Type II bursts for which the herringbone structure extends to the lowest frequency observable from the ground.

Cane *et al.* (1981) proposed an interpretation of the SA events in terms of acceleration of electrons at a Type II shock front, followed by their escape ahead of the shock to form a Type-III-like electron stream. This idea (Fig. 13.4) is analogous to a currently favoured qualitative interpretation of the herringbone structure in Type II bursts. It is thought that electrons are accelerated to >10 keV in shock fronts and then escape ahead and behind, to generate Type-III-like emission with the characteristic herringbone spectral structure.

Cane *et al.* (1981) found that 35 of 42 observed SA events were associated with high-energy particle events detected near the Earth's

orbit, and that for six of the remaining seven events the flare sites were not magnetically connected to the observation site (so that the detection of a particle event would not be expected). They concluded that: (i) SA events are associated with the more energetic (e.g. Type II/Type IV) events in the corona; (ii) if a shock is strong enough to produce Type II emission in the interplanetary medium then it is also strong enough to accelerate particles low in the corona; and (iii) the shock-accelerated electrons and the energetic particles from low in the corona have access to open field lines.

Interplanetary shock waves

The plasma-wave instrument on ISEE-3 has been used to study plasma turbulence associated with interplanetary shocks (Kennel *et al.* 1982). Most interplanetary shocks do not produce Type II bursts, and one might have hoped that this study of shock properties would shed light on the particular features which cause some shocks to generate Type II bursts while most do not. However, Type II bursts fade rapidly with distance from the Sun and cannot be detected above the galactic background beyond about 0.7 AU; consequently it has not yet been possible to identify and study as a distinct class those interplanetary shocks which produce Type II emission. Shock parameters may be calculated from measurements ahead of and behind the shock. These parameters are related by 'jump' conditions, which are generalizations of the familiar Rankine-Hugoniot

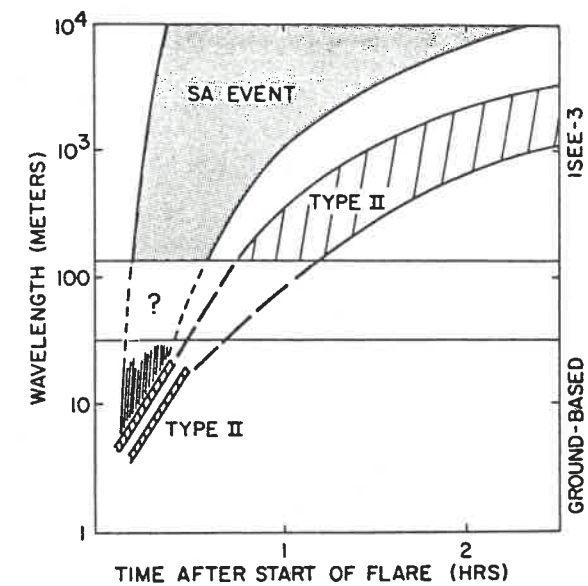


Fig. 13.4 - A schematic representation of the relation between metre-wavelength Type II activity with herringbone structure and the activity observed at kilometre wavelengths. Only the long-wavelength elements of the herringbone structure are shown. Note the absence of such structure on the Type II burst at kilometre wavelengths. (From Cane *et al.* 1981.)

relations for gas dynamic shocks (Zeldovich & Raizer 1966). An algorithm allows one to calculate the angle θ_{Bn} between the shock normal and the upstream magnetic field, the upstream β (the ratio of thermal and magnetic energy densities), and the Mach number M_F (the shock speed relative to the fast mode wave speed). The term 'upstream' refers to the region ahead of the shock. The upstream plasma can be considered as flowing into the shock. For 10 shocks reported by Kennell *et al.* (1982) θ_{Bn} ranged from 26° to 88° , β from 0.2 to 3 and M_F from 1.3 to 4.7. The angle θ_{Bn} is used to classify shocks as *quasi-parallel* for $\theta_{Bn} < 50^\circ$ and *quasi-perpendicular* for $\theta_{Bn} > 50^\circ$. Another classification is *sub-critical* for $M_F < 2.5$ and *super-critical* for $M_F > 2.5$; ions are strongly heated in super-critical shocks (Formisano 1977, 1981).

Kennell *et al.* (1982) found that ion-sound turbulence is present for several hours upstream from quasi-parallel shocks. Low-frequency electrostatic noise, whistler turbulence and a high-frequency ($>f_p$) continuum were found near each shock and for up to several hours downstream. From the viewpoint of theories of Type II bursts, the most relevant observation is the presence of Langmuir turbulence. Although no Type II bursts were observed at 1 AU, intense impulsive Langmuir waves were observed about an hour upstream from one shock, and impulsive Langmuir waves were present for a few minutes on either side of other shocks. The absence of a more extensive region of Langmuir turbulence is consistent with the absence of Type II bursts.

From the viewpoint of understanding the plasma processes involved in Type II emission these results are tantalizing. Langmuir waves and ion-sound waves are observed, but the Langmuir waves are not extensive enough to produce Type II emission. Moreover, it is not clear how the Langmuir waves are generated and why they are present in some shocks but not in others.

13.5 NATURE OF THE EXCITING AGENCY FOR TYPE II BURSTS

As we have already seen, there seems no doubt that the exciting agency for Type II bursts is an MHD-like shock wave - i.e. a disturbance with properties as predicted using MHD theory. However, the details of the structure of the shock and of its driver are not clear and there is no firm agreement on the interpretations of band splitting and of multiple lanes in Type II bursts.

Blast wave or driven shock wave?

A shock wave is usually described as being driven by a piston. In the case of a solar flare the piston is a mass motion resulting in some way from the flare itself. If this mass motion is fast enough, i.e. super-Alfvénic, a stand-off driven shock forms ahead of it. On the other hand, if the piston is slow, or if it is 'turned off' after a time, the initial shock disturbance proceeds as a blast wave.

It is proposed by McLean (1959) that Type II shocks are driven by an ejected mass of gas. The observation that many Type II bursts are closely correlated with coronal transients with speeds $>400 \text{ km s}^{-1}$

provides general support for this view. At first sight it seems plausible that the exciting agency for Type II bursts is a stand-off shock ahead of a coronal transient which is moving at nearly the Alfvén speed. However, as discussed in Section 13.2, detailed observations do not support this view. It seems that, in some cases at least, the Type II exciter moves faster than the coronal transient. In other cases either the Type II or the transient is not observed, so that the relation between them, if any, is not obvious. On average, the speeds of coronal transients, the speed of Type II bursts and the Alfvén speed in the corona ahead of the transient are certainly all of the same order.

An alternative interpretation in terms of a blast wave was proposed by Uchida (1974). The important qualitative difference between a driven shock and a blast wave is in the motions. A driven shock is tied to the motion of its driver. A blast wave has a wavefront the normal to which changes in accord with geometric optics; the normal to the wavefront is refracted as though the blast wave were a small-amplitude wavepacket. Observations which require motion along curved paths or refraction into regions of low V_A therefore favour the blast wave interpretation.

Uchida (1974) proposed that the refraction and focusing of an MHD blast wave in regions of low V_A could account for the details of the observed structures in multiple-lane Type II bursts. To determine the effects of refraction and focusing he used for the coronal magnetic field a model which was calculated from the measured photospheric field. The assumption that low- V_A regions become visible at $f = f_p$ or $2f_p$ as the blast wave passes provides a plausible interpretation of the structure and motion of a Type II burst. That is, the radiation comes only from the low- V_A regions, where the shock has a relatively large Mach number, while the surrounding high- V_A regions remain invisible.

Kai (1969a) reported an observation which has a natural explanation in terms of Uchida's (1974) model; a Type II burst appeared to be stopped or reflected at a region of strong magnetic field to one side of a flare. The inference that the shock could not propagate across the strong-field region is consistent with refraction away from regions of large V_A . Further evidence of refraction into low- V_A regions comes from Uchida's (1968) 'sweeping skirt' model for Moreton waves (Section 13.2). One class of observation which suggests motion along curved paths is the study of Type II bursts in cases where the flare occurred behind the limb. McLean (1980) listed four such examples.

It is quite likely that Type II bursts are produced at different times both by piston-driven shocks and by blast waves. Certainly Type II bursts are frequently observed in the absence of a suitable piston, i.e. in the absence of a coronal transient. On these occasions a blast wave interpretation seems appropriate. On the other hand, it is not at present clear whether Type II bursts ever occur in the absence of a suitable source for a blast wave, i.e. in the absence of a flare. Observations which show Type II bursts accompanied by coronal transients and eruptive prominences in the absence of a flare all relate to events

on or behind the limb, so that the occurrence of a flare cannot be excluded. On the other hand, there are numerous cases of coronal transients which are fast enough to produce a stand-off shock but which are not accompanied by a Type II burst.

Parallel or perpendicular propagation?

Early theories for collisionless shocks required that the shock propagate nearly perpendicular to the field lines (Tidman & Krall 1971). A number of theories for Type II bursts were developed on the basis of such models for collisionless shocks. The question whether the shock associated with the Type II is or is not perpendicular then became important from a theoretical viewpoint. More recent developments in the theory of collisionless shocks allow propagation at other angles and so this question has now become less important.

There is no clear observational evidence that the exciting agency for Type II bursts is restricted to nearly perpendicular propagation. Dulk *et al.* (1971) examined data for a number of Type II events but were unable to draw any firm conclusions as to the direction of propagation relative to the magnetic field. However, they considered that, on the available evidence, propagation is likely to be more nearly parallel than perpendicular. One argument to support this conclusion is that the positions of Type II and Type III bursts often coincide, and Type III bursts are certainly guided along magnetic field lines. Another argument is that the motion of Type II bursts which extend to low frequencies must have a substantial radial component, and over much of the path the magnetic field must also have a substantial radial component. Uchida's (1960) model for the propagation of a blast wave (see above) leads one to conclude that the criterion for the occurrence of Type II emission involves the value of V_A (emission is from low- V_A regions) and not the direction of shock propagation.

We conclude that the observational evidence is not consistent with strictly perpendicular shock propagation for all Type II events and that the range of shock angles over which Type II bursts can be produced is in fact quite large.

Split bands - interpretations

Early interpretations of the splitting of fundamental and harmonic bands involved magnetic splitting or Doppler splitting. Neither is satisfactory (Wild & Smerd 1972); magnetic splitting in some cases requires unacceptably strong magnetic fields, and Doppler splitting requires a current which would cause electrons to flow at unacceptably high speed relative to ions in a laminar shock model.

McLean (1967) proposed an interpretation in terms of a local inhomogeneous structure in the corona. The parts of the shock front which are parallel to the surfaces of constant electron density should emit intensely at a single frequency whereas the emission from other parts of the shock front will be spread thinly across a range of frequencies. McLean analysed an idealized quantitative model for a shock encountering a streamer and found that the simulated dynamic spectrum resembled a

split-band Type II burst. A variant of McLean's mechanism could explain split bands in terms of emission from two related low V_A regions in Uchida's (1974) blast wave model.

Smerd *et al.* (1974) suggested that the two bands correspond to emission in front of and behind the shock front. The electron density jumps at a shock front by a factor related to the shock Mach number M_A ; Smerd *et al.* estimated that values in the range $M_A \approx 1.2$ to 1.7 (which are plausible) are sufficient to account for the observed splitting.

Observations of slightly different positions for the two components of split bands have been interpreted as evidence in favour of McLean's (1967) model (Wild & Smerd 1972). However, Smerd *et al.* (1974) pointed out that at a fixed frequency the components from the two sides of a shock front would be emitted at different times. Nelson & Robinson's (1975) inference that the L source is further from the Sun than the U source at the same time is qualitatively consistent with the mechanism proposed by Smerd *et al.*

Both these mechanisms involve emission from two adjacent regions and the essential difference between them is that McLean's (1967) model involves splitting of the shock front and Smerd *et al.*'s (1974) model involves emission on both sides of a single shock. No definitive test to choose between the two mechanisms has been devised.

Starting frequency of Type II bursts

Whether the Type II exciter is a blast wave or a piston-driven shock, it is clear that its speed relative to the local Alfvén speed is important in determining the strength of the shock and the resultant radio emission. In an idealized corona with only a global dipole magnetic field and plasma distributed in height (h) according to a Saito *et al.* (1977) model, the Alfvén speed would be approximately constant with height, because V_A is proportional to f_B/f_p and in this idealized case both the gyro and plasma frequencies vary as $(R_\odot+h)^{-3}$. However, above active regions, where flares occur, the magnetic field is much stronger than the quiescent value and falls off more rapidly with height. Hence the Alfvén speed is very high (several thousand kilometres per second) in the low corona above these regions, but decreases over a few tenths of a solar radius to a nearly constant value of several hundred kilometres per second.

A Type II exciter launched in the vicinity of a flare is therefore likely to remain sub-Alfvénic while it traverses the high- V_A region low in the corona. Only in the lower- V_A regions, higher in the corona, does it become super-Alfvénic, with the resultant formation of a shock wave. This could account for the delay in the occurrence of the Type II burst after the start of the flare and its relatively low starting frequency. In contrast, Type III bursts usually begin at the time of the flare and at much higher frequencies than the Type II.

A related question is what happens to the Type II exciter further out in the corona after the radio emission has ceased. As mentioned

previously, most Type II bursts end at frequencies about 20 MHz. Robinson *et al.* (1984) have observed that three bursts which extend below 20 MHz (and continue on to become interplanetary Type II bursts) also start at lower than normal frequencies. It may be conjectured that the bursts which end above 20 MHz are due to blast waves which, according to Uchida's (1974) model, are strong enough to produce Type II emission only when they are focused into low- V_A regions. After reaching a region of nearly constant V_A they are no longer focused but disperse and weaken. Alternatively, the blast waves may become sub-Alfvénic as they move into regions of increasing solar wind speed, since their speed relative to the plasma then decreases. On the other hand, Type II bursts which start at very low frequencies may be due to piston-driven shocks. Two effects may allow the piston to remain sub-Alfvénic until it has risen very high in the corona: either it has a low constant velocity and V_A decreases outward, or it accelerates while it moves through the corona.

13.6 EMISSION PROCESSES FOR TYPE II BURSTS

We now assume that Type II bursts involve some form of plasma emission and that this emission process is related in some way to the passage of a shock wave or blast wave. Specific theories fall into three classes, depending on how the Langmuir waves are generated. The first class consists of Type-III-like theories in which the Langmuir waves are generated by streams of electrons. In the second class the Langmuir waves are generated in the shock front, and in the third class they are generated by a cloud of accelerated electrons which moves with the shock front.

Type-III-like theories

The first attempt at a quantitative theory for plasma emission was by Ginzburg & Zheleznyakov (1958), who applied their theory to both Type III and Type II bursts. We have already seen that the suggestion of a close analogy between Type II and Type III emission is consistent with observed properties, such as harmonic structure and polarization. The strongest argument for Type-III-like emission is the herringbone structure. The only explanation proposed for this feature is in terms of accelerated electrons escaping upstream and downstream from the shock front, and the recent identification of SA events (see Section 13.3) now provides direct evidence in support of this suggestion.

Another Type-III-like theory is due to Smith (1971, 1972a,b), who developed the theory of Type II emission based on the generation of ion-sound waves in a nearly perpendicular shock. Electrons are heated and accelerated by the ion-sound waves; they then stream away from the shock and generate Langmuir waves in a Type-III-like manner.

It is obvious that Type-III-like theories fail to explain either the backbone emission in sources with herringbone structure or the large class of Type II bursts which exhibit no herringbone structure. There has been no satisfactory suggestion as to how these difficulties can be overcome. Nevertheless, Type-III-like emission remains a favoured interpretation for Type II bursts.

Shock models

Before discussing the possibility of plasma emission from a collisionless shock front it is necessary to summarize the important features of relevant shock models.

Investigation of the theory of MHD shocks started in the early 1950s, and Bazer & Ericson (1959) introduced a classification in terms of MHD modes. Thus one speaks of fast, Alfvén or slow-mode shocks by analogy with the fast, Alfvén and slow MHD wave modes.

Development of the theory of collisionless shocks began with laminar shock models. The idea is to find a solitary-wave (soliton) solution and then to add to this the effect of some dissipation. As with MHD shocks, this leads to a classification in terms of wave modes, with ion-sound, magnetoacoustic and whistler solitons all leading to laminar shock solutions. The magnetoacoustic case is severely restricted, with the soliton solution existing only for nearly perpendicular propagation. This is unlike the collision-dominated case, in which there is no such restriction on fast-mode MHD shocks. Developments in the theory of collisionless shocks have been reviewed by Tidman & Krall (1971) and Biskamp (1973).

Other models of collisionless shocks may be described as 'turbulent' (Sagdeev 1966; Tidman & Krall 1971). Qualitatively, a turbulent shock corresponds to a shock structure in a regime where laminar models allow no shock structure and in which small-scale processes in the shock layer simulate the effect of collisions. In principle this can produce an MHD-like shock structure, the jump conditions being across the turbulent layer. In practice the difference in the electron and ion temperatures and the presence of energetic particles can play important roles in the shock structure. Indeed it is possible to have a shock transition in which the stresses are transmitted entirely by an energetic particle component, with the plasma parameters for the thermal plasma varying smoothly from the upstream to the downstream state (Drury & Völk 1981).

Observations of the Earth's bowshock (Greenstadt & Fredricks 1979) show that it is reasonably well described by the laminar model for nearly perpendicular propagation. When the shock normal direction is in the range $50^\circ \lesssim \theta_{Bn} \lesssim 80^\circ$ standing whistlers are observed upstream, at least for $\beta \ll 1$ and low Mach numbers $M_A \lesssim 3$. The range $\theta_{Bn} \gtrsim 50^\circ$ is called quasi-perpendicular propagation, and the shock structures are quasi-laminar in this range. Quasi-parallel shocks are turbulent. They are much thicker than quasi-perpendicular shocks, and involve multi-gradient magnetic profiles rather than a smooth well-defined magnetic profile.

One feature which may be relevant to Type II bursts is the fore-shock region. Electrons and ions reflected from or accelerated in the shock front populate a region upstream from the shock where wave turbulence in a variety of forms is found. Emission at the second harmonic of the plasma frequency from the streaming electrons is of particular

interest (Scarf *et al.* 1971). This emission is clearly plasma emission and seems to be analogous to interplanetary Type II emission which also comes from a foreshock region (Cane *et al.* 1982).

Emission from shock fronts

The second class of Type II emission mechanisms involves the generation of Langmuir waves in the shock front itself.

The earliest version of this class of mechanism is that due to Pikel'ner & Gintsburg (1964). Their idea is that in a perpendicular laminar shock the gradient in B through the front implies a current; if the current density is $j = N_e e v_d$, then for values of the electron drift velocity $v_d \gtrsim v_e$ the plasma is unstable to the generation of Langmuir waves because of the Buneman instability. This idea has been developed further by Zheleznyakov (1965), Zaitsev (1966) and Stepanov (1970). It was criticized by Smith (1971) on detailed grounds relating to the current profile, and Zaitsev (1977) replied to this criticism.

Current opinion does not favour this mechanism, but there seems to be no compelling argument against it. Perhaps the greatest difficulty is the fact that for $v_d > v_s$, where $v_s \approx v_e/43$ the current should be unstable to the generation of ion sound waves. The development of this ion-sound instability would prevent the Buneman instability from developing. That is, the growth of ion-sound waves would prevent v_d from exceeding a value near the ion-sound speed v_s . (Actually the ion-sound instability requires $T_e \gg T_i$ but there are analogous instabilities for $T_e \lesssim T_i$, e.g. those involving ion-cyclotron waves.)

Klinkhamer & Kuijpers (1981) suggested that the ion-sound waves might produce Langmuir waves through turbulent bremsstrahlung (Tsyrovich *et al.* 1975; Kuijpers 1980b). This would allow the Langmuir waves to be produced in the shock front itself. However, the turbulent bremsstrahlung mechanism itself has been the subject of controversy (Vlahos & Papadopoulos 1979, 1982; Kuijpers 1980c; Tsyrovich *et al.* 1981; Nambu 1981; Melrose 1982a), and it has been recently shown (Kuijpers & Melrose 1984; Melrose & Kuijpers 1984) that turbulent bremsstrahlung does not exist.

Observations of Type II bursts in the interplanetary medium generally indicate generation ahead of the shock rather than in the shock front itself. However, the data on interplanetary Type II events are only relevant to the interpretation of Type II bursts in the corona if the emission mechanisms are the same, and it is not clear whether they are. For Type II bursts at $\gtrsim 20$ MHz there is no direct evidence against emission from the shock itself or from behind (i.e. downstream from) the shock.

Emission from a co-moving cloud of electrons

The third class of Type II theories involves emission from Langmuir waves generated by a co-moving cloud of accelerated electrons. In this case the Langmuir waves are in balance between emission and

absorption by the energetic electrons. Tidman (1965) assumed that the accelerated electrons have a Maxwellian distribution; however, Melrose (1970b) showed that the resulting emission is then too weak to explain the observed brightness temperatures. Melrose (1975b), following Tidman & Dupree (1965), suggested that sufficiently bright emission could result if the electrons have a gap distribution (i.e. an isotropic distribution in which $f(v)$ has a minimum (with $f(v) \approx 0$) and a secondary peak at some suprathermal speed $v = v_0$). More recently this idea has been applied to emission at the second harmonic of the plasma frequency by electrons accelerated at the Earth's bowshock region and streaming back towards the Sun (Fung *et al.* 1982).

The analysis of emission from a gap distribution is very simple if the various stages reach saturation. As shown in Section 8.5, the maximum brightness temperature of the Langmuir waves is $T_L = m_e c^2 / 2K$ and the maximum brightness temperature of the second-harmonic radiation is $T_t = 2T_L$. It follows that this mechanism leads to $T_t \leq m_e c^2 / K \approx 10^{10}$ K.

We conclude that the emission mechanism for Type II bursts has not been clearly identified. There is strong evidence that the herringbone structure is due to Type-III-like emission from electrons accelerated in the shock front which escape into larger regions ahead of and behind the shock. Other mechanisms which differ in some essential way from Type-III-like emission encounter difficulties. This leaves us with no plausible theory for the emission from the backbone of the herringbone structure and from Type II bursts with no herringbone structure.

One possible mechanism involves a gap distribution which can be formed by electrons escaping ahead of (or behind) the shock. However, this mechanism cannot account (at least with isotropic electrons) for very bright ($> 10^{10}$ K) second-harmonic emission. Brighter emission requires anisotropic electrons which lead to an instability for the Langmuir waves.

13.7 ACCELERATION OF PARTICLES AT SHOCK FRONTS

Two-stage acceleration

Until quite recently there has been qualitative agreement between theory and observation on the need for two acceleration mechanisms, a faster one accelerating electrons to $\lesssim 100$ keV and a slower one accelerating ions and relativistic electrons. The theories which seem most likely to succeed in explaining acceleration of particles to relativistic energies generally require as input a population of suprathermal particles. Hence if these theories are applicable they can only be the second stage of a two-stage process. Phenomena associated with solar flares generally reveal two different time scales. At the impulsive phase of a flare we have ample evidence of the acceleration of electrons to energies $\lesssim 100$ keV in a few seconds (Type III bursts, impulsive microwave bursts, hard X-ray bursts). Type II bursts and the various continuum events (metre, decimetre and microwave), as well as the slower X-ray events, all come later in the flare, with a longer time scale. It has been believed that the impulsive stage of the flare corresponds

to the first stage of acceleration required by the theory, and that the sub-relativistic electrons accelerated at this stage are then further accelerated in a second stage to energies sufficient to explain the slower phenomena and also the energetic protons observed directly from space vehicles at 1 AU. However, it is now known from observations of γ -ray bursts that electrons with energies up to 1 MeV or more and energetic protons with energies ≥ 30 MeV can be accelerated in about 2 s. Hence if there are two stages of acceleration they can no longer be identified with the two major time scales of solar bursts.

Acceleration mechanisms

It is appropriate to comment briefly here on the development of ideas on the acceleration of particles in the wider context of all astrophysical plasmas. By the mid 1960s most of the acceleration mechanisms now known - i.e. various forms of stochastic acceleration and acceleration at shocks - had been proposed in one form or another, but the predicted low efficiency of these processes presented difficulties. Between 1960 and 1965 however it became recognized that fast particles could be scattered very efficiently by resonant interactions with whistlers (for electrons) or hydromagnetic waves (for ions). Efficient scattering makes a 'gas' of energetic particles act like a viscous fluid with negligible inertia compared to the background plasma. As a consequence energy exchange between turbulent motions and energetic particles can lead to a rapid damping of the turbulence, with most or all of the energy going into acceleration of the energetic particles. Such stochastic acceleration mechanisms are favoured for second-phase acceleration in the solar corona, as well as in many other contexts. First-phase acceleration is not of this type and is thought to be due to damping of electrostatic (ion-sound or Langmuir) turbulence.

In the late 1970s there was renewed interest in acceleration at shock fronts. This was motivated, on the one hand, by evidence of 'shock spikes' (spiky particle events associated with interplanetary shocks) and, on the other hand, by a new model for the interstellar medium which allows supernova shock waves to propagate over great distances and give up their energy by accelerating cosmic rays.

In discussing acceleration by shock waves we start with an older idea known as first-order Fermi acceleration and then show how this relates to the more recent ideas on acceleration at shock fronts. Next we discuss the energy changes which occur when a particle crosses or is reflected from a shock front; this leads to the so-called 'shock drift acceleration'. Finally we discuss possible 'first phase' mechanisms in a shock front.

First-order Fermi acceleration

The term 'Fermi acceleration' is used in a variety of senses ranging from a generic name for any stochastic acceleration mechanism to the specific mechanism proposed by Fermi (1949) himself. Fermi's original mechanism involved the reflection of cosmic rays from moving magnetized clouds. A head-on reflection leads to an energy gain and an overtaking reflection leads to an energy loss; a net average

acceleration occurs because head-on collisions are more probable than overtaking collisions. (This is the case only if the cosmic rays remain isotropic, and isotropy is achieved in Fermi's model by an assumption that the encounters occur at random angles; in more sophisticated models this implicit scattering mechanism needs to be replaced by an explicit scattering mechanism.)

The efficiency of Fermi-type acceleration is greatly enhanced by allowing only head-on collisions; such mechanisms are called first-order Fermi mechanisms. An example is illustrated in Figure 13.5.

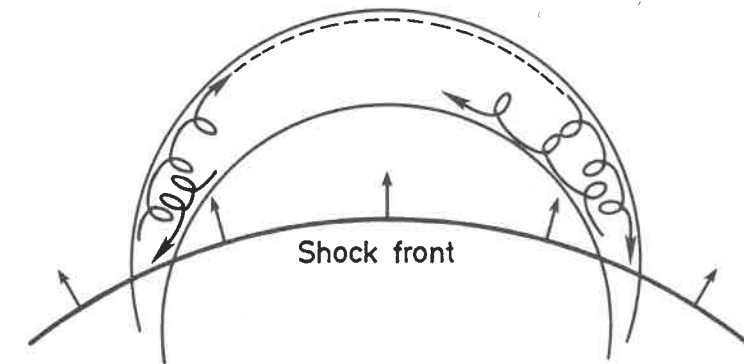


Fig. 13.5 - A model of first-order Fermi acceleration. As the shock front moves towards the top of the magnetic loop, electrons are accelerated by reflection from the shock at one side of the loop and then at the other. The energy is increased only in the direction parallel to the field at each reflection. Provided therefore that there is no scattering in the loop the pitch angles of the accelerated electrons systematically decrease.

A shock wave propagates towards the top of a flux loop in which energetic particles are trapped. These particles can reflect from the shock front. Every reflection is head-on and hence leads to a net energy gain for the particle. Of course this acceleration is necessarily of finite duration owing to the finite propagation time of the shock across the flux loop. A further difficulty, discussed by Wentzel (1964), arises because the probability of reflection depends on the pitch angle α of the particle and goes to zero as α goes to zero. Now each reflection increases the parallel energy with no change in the perpendicular energy, and hence leads to a decrease in α . Thus each reflection makes a further reflection less probable, and places a limit on the efficiency of the mechanism.

Resonant scattering of the trapped particle can offset the systematic decrease in α , and can, at least in principle, maintain a nearly isotropic distribution. In this way the scattering process acts as an effective stochastic mechanism and enhances the efficiency of the acceleration. However, as we now discuss, once one invokes efficient

scattering it is no longer necessary to appeal to a specific geometry to obtain first-order Fermi acceleration, i.e. one no longer needs to postulate two advancing shock fronts.

Diffusive acceleration at shocks

Suppose that energetic particles are scattered efficiently by scattering centres both ahead of and behind a shock front, and that the fast particles can freely cross the shock front. If the scattering centres are at rest with respect to the plasma around them, then the downstream scattering centres are approaching when viewed from the upstream ones, and vice versa. An energetic particle bouncing forwards and backwards between the two is always reflected head-on and hence experiences a first-order Fermi acceleration. The Alfvén waves required for the upstream scattering can be generated by the energetic particles themselves. The relevant instability is driven by the density gradient in the energetic particles ahead of the shock (strictly, the instability is driven by a pitch-angle anisotropy which is associated directly with the density gradient). The possibility of such 'diffusive' acceleration at shocks was pointed out independently by several different authors at about the same time - see the reviews by Toptyghin (1980), Axford (1981) and Drury (1983).

Diffusive shock acceleration is now favoured as the acceleration mechanism for galactic cosmic rays. Its role in accelerating particles in the solar corona and the interplanetary medium is less clear. There is in the solar case direct evidence for shock drift acceleration, discussed below, and it is possible that virtually all the acceleration is due to the latter mechanism. Shock drift acceleration is however ineffective for relativistic particles, and therefore it may well be that diffusive shock acceleration is important at high energies.

One problem with diffusive shock acceleration (and indeed with nearly all acceleration mechanisms) is that it requires 'seed' particles; the mechanism accelerates only particles which are already suprathermal. Specifically, the resonant scattering requires ions with speeds $\gg v_A$ or electrons with speeds $\gg 43v_A$. The passage of a shock can dump energy into such particles but diffusive acceleration alone cannot increase the number of such particles. Pre-acceleration is therefore required to provide the seed particles. The question of what mechanisms are involved in pre-acceleration has not yet been adequately explored.

Shock drift acceleration of ions

Shock drift acceleration occurs in models for oblique, nearly perpendicular laminar shocks. The obliqueness implies the presence of an electric field $\mathbf{E} = -\mathbf{v}_1 \times \mathbf{B}_1$ in the shock frame, where subscript 1 denotes values upstream. In the shock front itself the gradient in B causes a particle to drift (the 'grad B drift') at the velocity

$$\mathbf{v}^B = -\frac{m v_\perp^2}{2q} \frac{\text{grad } B \times B}{B^2} \quad (2)$$

Now, $q\mathbf{v}^B \cdot \mathbf{E}$ can be positive, and when this is the case all particles gain energy from the shock on interacting with it.

Shock drift acceleration is particularly favourable for the interpretation of shock spike events associated with interplanetary shocks and analogous phenomena associated with the Earth's bowshock (see e.g. reviews by Armstrong *et al.* 1977; Toptyghin 1980; Axford 1981; Pesses *et al.* 1982). The theory implies that upstream particles reflected back ahead of the shock should be highly collimated along B_1 , and this is a characteristic feature of observed shock spike events.

Another feature of the single particle dynamics is that when particles cross the shock front their first adiabatic invariant is conserved, at least approximately:

$$\left(\frac{p_\perp^2}{B} \right)_1 = \left(\frac{p_\perp^2}{B} \right)_2, \quad (3)$$

where subscript 2 refers to the downstream state. Using this equality and elementary properties of the shock it is possible to derive expressions for the changes in pitch and energy for each of the possible interactions (e.g. Toptyghin 1980). For non-relativistic particles the maximum kinetic energies are:

Reflection (1→1)

$$\frac{\epsilon_r}{\epsilon_i} = 1 + 4 \left(\frac{B_2}{B_1} - 1 \right); \quad (4)$$

Transmission (1→2)

$$\frac{\epsilon_t}{\epsilon_i} = 1 + 2 \left(\frac{B_2}{B_1} - 1 \right); \quad (5)$$

Transmission (2→1)

$$\frac{\epsilon_t}{\epsilon_i} = 1 + \left(\frac{B_1}{B_2} \right)^{\frac{1}{2}} + \left(1 - \frac{B_1}{B_2} \right)^{\frac{1}{2}}, \quad (6)$$

where i , r and t refer to incident, reflected and transmitted, respectively. The maximum value of B_2/B_1 is 4, and for a shock close to this maximum the energy of reflected and transmitted (1→2) particles can be increased manyfold.

Shock drift acceleration of electrons

The observations of shock spike events and the theory of shock drift acceleration refer to ions. However, it was reported by Potter (1981) that observations of 2 keV electrons by instruments on ISEE-3 showed increases in particle density by factors of 2 to 3 and sometimes >10 on passage of an interplanetary shock. The pitch-angle distributions for these electrons agreed with the signatures expected for shock drift acceleration. Potter pointed out that, although the argument in the case of electrons differs in detail from that for ions, one expects electrons, like ions, to conserve the first adiabatic invariant on crossing the shock. The treatment of shock drift acceleration for ions then also applies to electrons.

Holman & Pesses (1983) have developed a model for shock drift acceleration of electrons in connection with Type II bursts. This idea is as yet not fully developed and although it appears promising the question of the seed population remains; like diffusive shock acceleration, shock drift acceleration is effective only for suprathermal particles. Holman & Pesses suggested that acceleration of the electrons in the tail of a Maxwellian distribution may be adequate, but the source of the suprathermal electrons requires further investigation.

Acceleration by electrostatic turbulence

Electrostatic turbulence in the form of ion-sound waves is predicted in most turbulent-shock models, and is found to be associated with interplanetary shocks (Kennel *et al.* 1982). Ion-sound turbulence (for $T_e \gg T_i$) damps by heating electrons and this heating is a possible candidate for the mechanism of first-phase acceleration. The major uncertainty with this mechanism concerns the time scale for effective heating compared with the time scale for escape of the electrons from the shock front. If electrons remain in the front long enough to be heated to $\sim 10^8$ K, at least in some regions, then escape of such electrons could account for the observed herringbone structure and SA events.

If the electrostatic turbulence includes Langmuir waves, then the latter damp by accelerating electrons. Langmuir waves with phase speed $v_\phi \approx \omega_p/k$ accelerate electrons with $v \geq v_\phi$. Unlike ion-sound waves, most of the energy in Langmuir waves can be deposited in a suprathermal electron component. (Ion-sound waves have $v_\phi \ll V_e$ and accelerate virtually all electrons; this is equivalent to saying that they damp by heating the electrons.) However, there is no direct evidence that a major fraction of the free energy goes into Langmuir turbulence, and it seems likely that any turbulent acceleration is due predominantly to ion-sound waves.

Turbulent heating by ion-sound waves and shock drift acceleration seem the two most plausible alternative mechanisms for accelerating the electrons which produce the herringbone structure and SA events. Further observational data on interplanetary shocks and further analysis of the two mechanisms will be required before we can determine which is the more favourable.

In summary: there are several different mechanisms which could lead to acceleration of electrons at or in association with shock fronts. Shock drift acceleration has attractive features for the interpretation of herringbone structures. Diffusive acceleration probably occurs but it is important only for particles of higher energy than those thought to be involved directly in Type II emission. Acceleration by ion-sound turbulence is not favourable and acceleration by Langmuir turbulence, although favourable in principle, requires a source of Langmuir turbulence other than the energetic electrons themselves; the only likely source suggested has been turbulent bremsstrahlung, which has now been shown not to exist (Kuijpers & Melrose 1984; Melrose & Kuijpers 1984).

13.8 CONCLUSIONS

On a superficial level Type II bursts may be explained in terms of plasma emission associated with an MHD-like shock front generated in association with a sufficiently strong solar flare. However, many of the Type II emission phenomena are not understood in detail. The relation between the Type II exciter and the outwardly moving mass ejected in the coronal transient is not clear. In the interplanetary medium it seems that the Type II emission comes from well ahead of the shock, and yet in at least one popular theory (for band splitting of the bursts from the lower corona) emission comes from both in front of and behind the shock. The details of the emission mechanism also remain uncertain. Some features, notably the herringbone structure, can be explained in terms of Type-III-like emission caused by streams emanating from the shock front. However, not all Type II emission is of this type; some Type II emission is smooth with no evidence of Type-III-like electron streams. Finally, it is not clear why some shocks in the interplanetary medium lead to Type II emission while others do not; the explanation is probably connected with the details of the acceleration mechanism for electrons at the shock front.

In brief, ideas relating to Type II emission are continually being updated, but we still have not clearly identified all the important processes involved.